ITCZ breakdown in three-dimensional flows

Chia-chi Wang and

Gudrun Magnusdottir*

Department of Earth System Science,

University of California, Irvine.

September 14, 2004

*Corresponding author address:
Prof. Gudrun Magnusdottir
Department of Earth System Science
University of California, Irvine
Irvine, CA 92697-3100 email: gudrun@uci.edu

Abstract

The ITCZ (Intertropical Convergence Zone) is observed to undulate and at times break down into a series of tropical disturbances in several days. Some of these disturbances may develop into tropical cyclones and move to higher latitudes while others dissipate, and the ITCZ may reform in the original region. It has been proposed that the ITCZ may break down due to its heating induced potential vorticity (PV) anomalies. Here this process is examined in three dimensional simulations using a primitive-equation model. A simulation of the ITCZ in a background state of rest is compared to simulations in different background flows. The effect of different vertical structures of the prescribed heating is also examined.

Deep heating induces a positive PV anomaly in the lower troposphere, leading to a reversal of the PV gradient on the poleward side of the heating, while the induced PV anomaly at upper levels is negative, leading to a reversal of the PV gradient on the equatorward side of the heating. The response at upper levels leads to a weaker PV gradient change, but the response is greater in areal extent, than the lower tropospheric response. For shallow heating, the lower tropospheric PV response is greater than that for deep heating and there is no upper tropospheric PV response. The ITCZ lasts longer before breaking in this case than in the deep heating case.

Effects of the background flow are mainly felt by the deep heating cases. When the background flow enforces the PV induced wind field, ITCZ breakdown occurs more rapidly, whereas when the background flow is opposite to the PV induced flow, ITCZ breakdown takes longer and the ITCZ may dissipate before breakdown.

1. Introduction

The Intertropical Convergence Zone (ITCZ) is a zonal belt of rather low pressure located in the tropics where there is low-level convergence, and cloudiness and precipitation are prevalent. The ITCZ has been observed to undulate and break down into a series of disturbances on satellite images (e.g., Agee 1972; Thompson and Miller 1976; Hack et al. 1989). Some of the disturbances may intensify and grow into tropical cyclones while others dissipate. After the produced disturbances move away toward higher latitudes, a new ITCZ may reform in the same general location. This process is referred to as "ITCZ breakdown" (Hack et al 1989; Schubert et al. 1991; Guinn and Schubert 1993; Nieto Ferreira and Schubert 1997, hereafter NFS).

The sequence of visible satellite images shown in Fig 1 is a case of ITCZ breakdown that occurred in the tropical eastern and central Pacific at the end of October 2002. The ITCZ started to undulate on 19 October and broke down on the 22nd. One of the disturbances located at approximately 11°N, 130°W (labeled as L) developed into a tropical cyclone named Lowell (22–31 October) while part of the ITCZ to the southeast of Hawaii continued breaking into more disturbances and, later on, one of them developed into hurricane Huko (labeled as H) at approximately 10°N, 155°W (10/24–11/03). After these tropical cyclones and disturbances moved away or dissipated, a new ITCZ reformed in the same area. The timescale of this entire process is typically 1–2 weeks. During this particular episode of ITCZ breaking, a hurricane, named Kenna (labeled

as K), developed near the west coast of Mexico (22–26 October). However, because of its proximity to the continent, it is likely that the formation of Kenna was strongly influenced by flow over the high topography of Mexico.

Dynamical processes that can cause the breakdown of the ITCZ in the tropical east Pacific and subsequent formation of tropical cyclones include the following two: (1) Propagation of easterly waves from the Atlantic and their interaction with the ITCZ (e.g., Avila and Clark 1989), (2) cyclogenesis due to interaction of the flow with the terrain of the Sierra Madre mountains of Mexico and subsequent interaction of the generated disturbances with the ITCZ (Zehnder and Powell 1999). The first above would allow tracking of disturbances at least back to the Caribbean, while the second usually only generates disturbances very close to the coast of Mexico that may interact with the easternmost part of the ITCZ. In some cases, no westward propagating disturbance precedes the breakdown of the entire ITCZ.

In the present work, we would like to focus on a third dynamical process that can lead to the breakdown of the ITCZ. This is the idea that the ITCZ is inherently a dynamical entity that may break down without interactions with any external disturbances. This mechanism of breakdown was first suggested by Charney (1963) and then expanded upon in several papers by Schubert and collaborators as we shall describe in section 2. "ITCZ breakdown" is the term used by Schubert and collaborators to describe the breakdown of the ITCZ due to its own instability. For historical reasons, we shall continue to use

that term in this paper, even though the term "vortex roll-up" of a potential vorticity (PV) strip might be more insightful. However, our numerical experiments are forced experiments, and the forcing itself plays an important role in the instability as will be discussed in section 4a. This distinguishes our experiments from the vortex roll-up mechanism, which does not involve any forcing.

ITCZ breakdown is an efficient mechanism for pooling vorticity in the tropical atmosphere in order to form disturbances that represent the early stages of tropical cyclogenesis. Here, we shall extend this idea in two directions. Firstly, we extend the barotropic modeling study of NFS to consider three dimensional simulations using the Reading spectral model. Observations of the vertical profile of heating in organized convection in the tropical east Pacific are very limited. Recent studies (e.g., Nesbitt et al 2000; Zhang et al 2004) suggest that shallow convection may be important. It is therefore of interest to examine the sensitivity of ITCZ breakdown to the vertical structure of the heating. Secondly, we examine the effect of nonzero background flow on the process of ITCZ breakdown.

The outline of the paper is as follows. Section 2 gives further details on the dynamical processes involved in ITCZ breakdown and reviews previous work. In section 3, we describe the model, the prescribed heating, and the different background flows that we use in the numerical experiments. Sections 4–6 contain results, in a background state of rest, idealized background flows, and a climatological background flow, respectively.

Section 7 contains concluding remarks.

2. Background

The idea of an inherent instability of the ITCZ, associated with its diabatic forcing, is straightforward. As discussed by Hoskins et al. (1985, §7) and further detailed by Hoskins (1991), a heat source in the free atmosphere will generate a positive PV anomaly below the maximum heating and a negative PV anomaly above. Since the background, latitudinal PV gradient is positive in the Northern Hemisphere (NH), given enough heating, the PV gradient on isentropic surfaces may change sign on the poleward (equatorward) side of the heating below (above) the maximum heating in the vertical. Thus, necessary conditions for instability may be satisfied in these two different regions of the flow.

Hack et al. (1989) used a (time-dependent) balanced, axisymmetric model to simulate the time evolution of the Hadley circulation when the flow is forced with a specified heating that is narrow in latitude, with a mid-tropospheric maximum. They found that in a matter of a couple of days, the heating had produced reversals of the PV gradient in the lower and the upper troposphere. The lower tropospheric PV gradient reversal (on the poleward side of the heating) was dominant. Thus, they hypothesized that there is nothing unique about the formation of easterly waves in the African region by instability of the lower tropospheric flow. Convection in the ITCZ can induce unstable

lower level flows in other tropical regions such as the east Pacific. Schubert et al. (1991) used potential temperature as the vertical coordinate in their balanced, axisymmetric model. They experimented with different vertical profiles of heating, reached the same conclusions as before, and hypothesized that in a couple of days the ITCZ can induce its own breakdown into tropical disturbances that could move away, allowing the ITCZ to reform and the process to start over again.

Barotropic aspects of ITCZ breakdown were subsequently examined thoroughly by NFS using a high-resolution shallow water model on the sphere. The most intriguing results of their study involve experiments with ITCZs that are zonally elongated but do not extend around all longitudes. They use a zonally extended (90° longitude) mass sink to simulate the lower tropospheric effects of the heating that leads to the ITCZ, letting the mass sink act during the first five days of simulation, then turning it off and watching the subsequent evolution of the flow. Breakdown of the ITCZ into three vortices occurred over the next week. The central vortex dominated the other two. All three vortices were located poleward of the forcing region, which is consistent with observations of tropical cyclones (Gray 1968). We have repeated many of NFS's experiments in the Reading shallow water model and we found that a resolution of T106 (approximately 1.1° by 1.1°) is sufficient for reproducing the salient features of their results (NFS use a resolution of T213). Here, we extend their results in a three dimensional primitive-equation (PE) model.

It is unfortunate that Hack et al. (1989), Guinn and Schubert (1993) and NFS all chose to show the same case of ITCZ breakdown (late July to early August 1988), perhaps giving the impression that this was an isolated incident, which it is not, at least for the east Pacific. Our confidence that ITCZ breakdown is indeed a valid mechanism for pooling vorticity in the tropical atmosphere, in particular in the east Pacific, arises from several points. Tropical-cyclone scientists who are particularly familiar with satellite products believe that ITCZ breakdown takes place routinely in the east Pacific during the warm season, especially in more shallow convection (Ray Zehr, personal communications 2002). Indeed, our own analysis of GOES satellite images over several seasons revealed a number of cases of ITCZ breakdown (one example is shown in Fig. 1). Additionally, from the newly available scatterometer data (e.g., Liu and Xie 2002), one can calculate vorticity and divergence of the surface wind and this has revealed matching structures with the GOES satellite images. The third independent satellite dataset that we consider is Tropical Rainfall Measuring Mission (TRMM) cloud liquid water content. This will be the subject of a forthcoming paper.

Any analysis products in the tropical east Pacific are going to be heavily influenced by the model used, due to the lack of radiosonde and other conventional observations in that area. Our own experience is that the standard resolution NCEP/NCAR reanalysis data (at 2.5° by 2.5°) is not able to depict PV strips corresponding to the ITCZ in the tropical Pacific. However, the high resolution NCEP global tropospheric analyses (at

1° by 1°) that has been available since Sept. 1999 does pick them up. Thus, it is not surprising that Sobel and Bretherton (1999) were unable to find vorticity strips at the 850 and 500 hPa levels in NCEP/NCAR reanalysis data.

Gu and Zhang (2002) in their comprehensive observational study of westward propagating synoptic scale disturbances and the ITCZ, found that the ITCZ breakdown hypothesis is consistent with their results. The disturbances tend to be located poleward of the ITCZ, which is consistent with the hypothesis. They also found that the relationship between the ITCZ and synoptic-scale disturbances varies zonally, having the closest correlations over the east Pacific. Of course, they were not specifically looking for incidences of ITCZ breakdown. Included in their results would be cases where an easterly wave propagates into the region and subsequently interacts with the ITCZ, which is not the mechanism of ITCZ breakdown that we are concentrating on here.

The tropical disturbances resulting from ITCZ breakdown are usually weak. They dissipate quickly if the environment is not favorable. That is also why this process has been largely ignored, except when one of the disturbances grows into a tropical depression.

3. Model, forcing and background flow

We use the Reading spectral PE model (Hoskins and Simmons 1975), at horizontal resolution of T106 (approximately 1.1° by 1.1°) with 10 equally spaced sigma levels

(0.05, 0.15, 0.25,...,0.95) in the vertical on an aqua-planet. Some of the experiments were performed at double this vertical resolution. Results for deep heating were found not to be sensitive to the vertical resolution. The mean temperature for each layer is the US standard annual mean temperature averaged over 15°N (U.S. Standard Atmosphere Supplements, 1966, p.98-99)[†]. The model has ∇^6 hyperdiffusion added to the vorticity, divergence and temperature tendency equations, with a decay rate of 10 day^{-1} for the smallest resolved horizontal scales.

Our numerical experiments are forced in that we apply thermal forcing (parameterized heating) over the first five days of simulation to generate the ITCZ and its associated PV anomalies. We then watch the evolution of the flow without this thermal forcing over the following 15 days. The thermal forcing is applied in a background state of rest, as well as in different background flows, which are themselves maintained by forcing the model. Each background flow is highly idealized.

The prescribed heating is ramped up in the first 12 hours of simulation. It is kept at full amplitude for the following 4 days, then turned off smoothly over the following 12 hours. The evolution of the flow is examined after day 5 when the heating has been turned off. Each experiment is integrated for a total of 20 days (15 days after heating is turned off). The horizontal profile of the heating is identical to that of NFS and is shown in Fig. 2a. It is elliptical in shape, spans 90° longitude and 5° latitude, and in all cases is centered on 10° N. This is the heating rate at 600 hPa where the heating is

[†]Publisher: U.S. Government Printing Office, Washington D.C. 20402

maximum in the vertical. The vertical profile of heating, termed deep heating, is shown in Fig. 2b. It is designed by two parabolas connected at 600 hPa. We experimented with different vertical structures of heating, but the horizontal and temporal structure was always the same.

The background flows are zonally symmetric. In each case, the model is initialized with a background flow that is maintained in steady state thereafter. As the flow evolves, given the prescribed heating, zonal asymmetries quickly develop. The background flows that we consider are either idealized or climatological. The two idealized background flows are generated by forcing the PE model with a zonally symmetric heating that has the same vertical structure as the profile in Fig. 2b and the same latitudinal structure as the central longitude in Fig. 2a. In one case, this heating is applied for 5 days at 10° N to generate the background flow that we term "the idealized trade wind case". In the other case, this heating is applied at 10° S to generate background flow for the experiment that we term "the idealized double ITCZ case". In both cases, at the end of 5 days we save the vorticity and divergence fields to use as background flow, which is maintained during simulation, in new experiments where the heating (shown in Fig. 2) is applied at 10° N. The left hand panel of Fig. 3 shows the background flow for the idealized trade wind experiment, and the right hand panel shows the background flow for the double ITCZ experiment. Note that since the latitude of the zonally symmetric forcing is symmetric about the equator in these two cases, the resulting fields are also

symmetric about the equator. Each panel shows zonal wind, meridional wind, and the horizontal flow on the 310 K isentropic surface, from top to bottom.

The climatological background flow is derived from high resolution NCEP global tropospheric analysis (horizontal resolution 1° by 1°). It is the time mean and zonal average of three active seasons in 2000, 2001 and 2002. We define the active season as lasting from August through October. This definition is based on our own analysis of ITCZ breakdown in this high resolution dataset as well as in satellite data over the tropical east Pacific. This background flow is depicted in Fig. 4.

4. Results for experiments in a background state of rest

Figures 5 and 6 show the evolution of ITCZ breakdown in a background state of rest on the 310 K (about 800 hPa) and 345 K (about 250 hPa) isentropic surfaces, respectively. These two isentropic surfaces intersect the main areas of response in the lower and upper troposphere, respectively. The region shown here is 10°S–30°N. Contours indicate the PV field in PVU (1 PVU=10^{-6} K m^2 s^{-1} kg^{-1}) and vectors indicate the corresponding horizontal wind field. A positive lower-tropospheric PV maximum (PV strip) is observed on day 5, when the forcing has just been turned off, as seen in Fig. 5a, on the poleward side of the heating, below the level of maximum heating. The PV strip has already developed a counter-clockwise tilt at this stage produced by the induced cyclonic wind field, but opposed by the latitudinal gradient of planetary vorticity. The

evolution of the low-level flow on days 7, 9 and 11 is shown in Figs. 5b–d. This evolution is qualitatively similar to that shown in Fig. 11 of NFS that depicts the response to a mass sink of the same horizontal shape with the same time dependence as the multilevel forcing in our PE model, but in that instance simulated in a single layer, shallow water model. By day 7 (Fig. 5b) the PV strip is already undulating. Note that the undulation and subsequent breaking starts from the western end of the strip. After the heating is turned off, PV is conserved (aside from the ∇^6 dissipation at the smallest horizontal scales). As the western end of the PV strip tilts toward equator, its planetary vorticity is decreased, the mass density in isentropic coordinates is increased and the relative vorticity must increase to conserve PV. This will induce increased cyclonic flow (including a cross-equatorial component) on the western end of the strip and spin up a vortex that may break off the PV strip.

The PV strip breaks down into three vortices on day 9 (Fig. 5c). On day 11 (Fig. 5d) the central and eastern vortices dominate the western one. Later in the simulation the central vortex dominates as the eastern one propagates away and weakens, and the western vortex is distorted and merges with the central one. The large-scale response in terms of a pressure perturbation is similar to that shown by Heckley and Gill (1984) in an idealized barotropic model of the time evolution of the response to enhanced forcing at 10° N. Figure 7 shows the response in pressure on the 310 K isentrope on day 7. The familiar signature of the equatorial Kelvin wave propagating to the east and two Rossby

waves on both sides of the equator propagating west is evident in the figure.

The PV produced by this heating at upper levels is opposite in sign, and the associated change in the latitudinal PV gradient is weaker than that in the lower troposphere. The maximum PV gradient change occurs equatorward of the maximum heating. The time evolution of the PV anomaly (where PV in the initial state is subtracted from the PV field) on the 345 K isentropic surface is shown in Fig. 6, on days corresponding to those in Fig. 5. Note that the upper level PV anomaly corresponding to the heating is more global in area extent than the PV anomaly in the lower troposphere. The wind perturbation appears to propagate rather quickly out of the region so that by day 11 it is confined to relative longitudes –90° and further west. This corresponds to the propagation of long Rossby waves (such as are evident in Fig. 7) out of the forcing region. We examined the response to a mass source (as opposed to a mass sink) in our shallow water equation model (all other parameters held fixed) and found that the response is similar to Fig. 6 in that it is weaker in amplitude, but more global in area extent, than the response to a mass sink.

a. Initial value problem vs. forced experiment

In forced experiments such as the one described above, the instability forms as a result of the heating and not as a result of an instability of a basic state flow. In these cases, the nature of the forcing is as important as the nature of the flow for determining

the flow instability (e.g., Andrews 1984). We compared an initial value experiment of a PV strip to a forced experiment where the same PV strip was generated by thermal forcing. To keep the experiments simple, the imposed heating is zonally symmetric with the same latitudinal, vertical and temporal dependence as the heating described in section 3. The PV strip on day 5 of the forced experiment was the same as the initial PV distribution in the initial value experiment. In both cases we added a small white noise perturbation to the surface pressure field and integrated for 40 days. Comparing the subsequent flow evolutions revealed some differences (not shown). For the initial value experiment the PV strip broke down into considerably weaker disturbances than those coming from the forced PV strip. The wavelength of the most unstable mode and thus the number of disturbances is also different in the two experiments. The initial value experiment is much like the typical barotropic instability study in that the wavelength of the most unstable mode is six times the width of the PV strip (e.g., Kuo 1973; Joly and Thorpe 1990). The wavelength of the most unstable mode in the forced experiment is longer. We find that the wavelength of instability selected for the forced experiment is 17% longer than the wavelength selected for the initial value experiment.

The above differences in flow stability between two experiments having exactly the same PV strip, which is imposed initially in the initial value experiment and thermally forced in the forced experiment, support the notion that the nature of the forcing has an effect on the stability of the flow. This applies also to the experiments described in

sections 5 and 6 where the thermal forcing is applied in a nonzero background flow.

b. Sensitivity experiments involving the vertical profile of heating

To better understand the sensitivity of the model response to the strength and structure of the vertical profile of heating, we performed four sets of sensitivity experiments by: (1) moving the peak heating in the vertical, (2) moving the bottom of the heating in the vertical, (3) increasing the maximum heating rate, and (4) making the heating shallower. The horizontal and temporal structure of the heating is constant in all experiments. Unlike some other numerical studies (e.g., Wu 2003), we did not fix the average heating rate over a vertical column. Rather, the value of the peak heating rate (in the vertical) was kept the same in each case. Since the strength of the induced PV in the lower troposphere is proportional to the vertical gradient of heating below the peak as shown in the following relation

$$\left(\frac{\partial P}{\partial t}\right)_\theta + \mathbf{v} \cdot \nabla_\theta P = -\dot{\theta}\frac{\partial P}{\partial \theta} + P\frac{\partial \dot{\theta}}{\partial \theta}, \tag{4.1}$$

we were most interested in varying this gradient. In the above, friction is neglected, P is PV, $\mathbf{v}$ is the horizontal velocity field on an isentropic surface, the ∇ operator is horizontal, θ is potential temperature and subscript θ means that derivatives are taken at constant θ. Indeed, we find that any change that increases this vertical gradient below

the peak heating, such as lowering the peak heating in the vertical, lifting the bottom of the heating curve, increasing the maximum heating, or making the heating profile shallower while maintaining the same maximum heating rate, will generate stronger lower tropospheric PV anomalies. However, the process of ITCZ breakdown need not be accelerated. In fact, we found that evolution of ITCZ breakdown is slower by one day when the heating is shallow (not shown).

The vertical heating profile for the shallow heating is shown in Fig. 8a (dashed), along with the deep heating profile (solid). The other experiments with increased rate of PV production due to the increased gradient of heating (not shown), had accelerated ITCZ breakdown. In the case of the shallow heating, the two terms on the right hand side of (4.1) cancel to a large extent above the maximum heating such that no negative PV anomaly is generated above the positive anomaly. This may contribute to the increased stability of this PV strip compared to the PV strip generated by deep heating. A meridional cross-section through the center of the PV anomaly generated by the shallow heating is shown in Fig. 8b, and through the center of the PV anomaly generated by the deep heating is shown in Fig. 8c. Both are snapshots taken after the heating has been turned off (day 5). Note the wide reaching, upper tropospheric PV anomaly in the deep heating case that is absent in the shallow heating case. The lower tropospheric PV anomaly in the shallow heating case is substantially stronger than the corresponding PV anomaly for the deep heating case.

Wu (2003) proposed that shallow heating may serve an important role in preconditioning the flow for the development of deep convection. The importance of organized shallow convection in the tropical east Pacific has recently been confirmed by Zhang et al. (2004) using four independent observational datasets. The shallow heating profile is therefore highly relevant.

We examined the vertical normal mode transform of the deep and shallow heating profiles, using the method of Fulton and Schubert (1985). We found that results for the deep heating profile were quite similar to the GATE disturbed heating profile (Fulton and Schubert 1985). The profile projects dominantly on the external mode and the first three internal modes. By contrast, the shallow profile projects the strongest on the external mode, and on the first 6 internal modes, with an order of magnitude less projection on the following few modes. Since most of the atmospheric energy projects onto the external mode (Kasahara and Puri 1981), the most important result is the number of internal modes that the heating projects prominently onto. The lower that this number is, the less complicated the vertical structure of the heating. With the more complicated vertical structure for the shallow heating, it is hard to argue for a clean separation of vertical modes in order to justify using a barotropic model to simulate the lower tropospheric response to the shallow heating. Such models have been widely used to simulate the tropical response to heating, but they may only be useful for deep heating.

5. Experiments with idealized background flows

Here we discuss the effects of two different background flows, described in section 3 and shown in Fig. 3, on ITCZ breakdown. Figure 9 shows the lower tropospheric time evolution of ITCZ breakdown in the idealized trade wind background flow and should be compared to Fig. 5, which shows the time evolution in a background state of rest. In both cases the heating inducing the ITCZ is deep. ITCZ breakdown is accelerated in the presence of the idealized trade wind background flow. This is consistent with Dritschel (1989) who showed for barotropic balanced flow that when cooperative shear is present, the vorticity strip becomes more unstable than in a background state of rest.

The behavior mentioned in the previous section, describing how a vortex rolls up from the western end of the PV strip first, is exaggerated by the cooperative shear as can be seen in Fig. 9. We found a case of ITCZ breakdown in the high resolution NCEP global tropospheric analyses data in summer 2000, which may have evolved in the same way. In this observational case, a relatively long PV strip was noticed in the region of the eastern tropical Pacific (80°W- 130°W, 5°N-10°N) on 24 August, 2000. This PV strip started to undulate, and as shown in Fig. 10, a piece of high PV broke off from the western end of the PV strip on 26 August. This vortex developed into a named tropical storm, John (8/28–9/01). The remaining part of the PV strip continued breaking down into a few small disturbances that dissipated quickly. The formation of tropical storm John has been confirmed to originate from disturbances within the ITCZ, in the absence

of easterly waves (Lawrence et al. 2001). The above modeling experiment suggests that cooperative shear of the background flow may be another factor boosting the roll up from the western end of the PV strip. Of course, in this particular case, other factors may simultaneously influence ITCZ breakdown, such as Rossby waves excited by the vortex west of the PV strip (around 15°N, 145°W) on 26 August. Note that this pre-existing vortex is not part of the PV strip, neither on 26 August (Fig. 10b) nor on 24 August (Fig. 10a) when it was located at (12°N, 133°W).

Over several days the trade winds may be significantly stronger than the idealized trade wind described above, in which case the difference in maximum windspeed between the equatorward westerlies and the poleward easterlies was 14 m/s. Therefore, we imposed trade winds with low-level difference in windspeed between the westerlies and easterlies of 22 m/s. In this strong trade-wind case (not shown) the ITCZ breakdown occurs faster. Again, the breaking starts from the west, but the rest of the PV strip breaks into several small disturbances, rather than the three larger disturbances seen in the weaker trade-wind background flow. This is more in line with the case from August 2000 shown above.

The idealized double ITCZ background flow was inspired by several observational studies of this phenomenon (e.g., Liu and Xie 2002, and references therein). The double ITCZ is most robust in the tropical east Pacific where it exists year round, being most evident in spring. For convenience, in this paper we refer to the convergence zone in the

NH (the dominant one) as the ITCZ, and the one in the Southern Hemisphere (SH) as the Southern Convergence Zone (SCZ). Results for a background flow corresponding to the idealized double ITCZ is shown in Fig. 11 in the latitude range 30°S to 30°N. The SCZ is initially zonally symmetric (in steady state), with fixed PV values as described in section 3. The ITCZ heating is then turned on for five days in the beginning of simulation. As the ITCZ develops, a low level cyclonic flow is induced. Thus, in this case, the background flow opposes the induced flow on the equatorward side of the ITCZ (adverse shear) and this stabilizes the PV strip. Eventually, a vortex breaks off the western end of the ITCZ, but the rest of the PV strip stays intact for several days longer, slowly dissipating without breaking apart. The results of this experiment are consistent with Dritchel's (1989) results for a vorticity strip in adverse shear. He found in a series of idealized numerical experiments for two-dimensional balanced flow on an f-plane that when the adverse shear is weak, the strip of vorticity is unstable. As the adverse shear increases, the shear overcomes the roll-up effect, and the strip undulates with diminishing amplitude. The shear about the ITCZ in the double ITCZ background flow is adverse on the equatorward edge of the ITCZ. At its poleward edge, the northeast trades are nearly in the same direction as the flow field induced by the ITCZ.

What is perhaps most interesting about this case is the strong influence of the ITCZ on the SCZ. As the vortex rolls up on the western end of the ITCZ, a stronger vortex, symmetric about the equator, rolls up on the SCZ. In fact, this SH vortex becomes

the dominant one in the subsequent evolution of the flow. This is partly due to the strong cooperative shear on the equatorward side of the SCZ PV strip due to the ITCZ, and partly due to the interaction between PV anomalies induced by the ITCZ and the SCZ. The PV response at upper levels is extensive in area (Fig. 8c). Figure 12 shows a meridional cross section of PV anomaly through the longitudinal center of the ITCZ in a double ITCZ background flow on day 0, before the heating generating the ITCZ is turned on, and on day 5 when this heating is turned off. PV anomaly is defined as the PV for the double ITCZ case on the day in question with PV on day 0 in a background flow of rest subtracted. As the prescribed heating in the NH ITCZ increases, the upper level divergent flow of the SCZ faces the outflow of the ITCZ near the equator and upward motion in the SCZ is substantially decreased. This downward anomaly in vertical motion in the SCZ then compresses the lower troposphere locally, leading to an increased lower tropospheric PV anomaly as can be seen in Fig. 12b. Later in the simulation, the SCZ east of the dominant vortex breaks down into several disturbances as can be seen in Fig. 11d.

When the vertical structure of the ITCZ heating is changed from deep to shallow, there is less interaction between the ITCZ and the SCZ as the upper tropospheric PV anomaly is absent for shallow heating. The results are shown in Figure 13. The ITCZ breaks down, as was the case when there was no background flow. At the same time, while still influenced by cross-equatorial flow of the ITCZ, which is of limited longitudinal

extent, the SCZ breaks down into weaker disturbances.

We also examined ITCZ breakdown in a stronger double ITCZ background flow, where again we consider deep heating in the ITCZ. In the stronger background flow, the ITCZ is stabilized by the adverse shear and it does not break at all. Instead it stays in place until finally dissipating on day 12. At the same time, the southern convergence zone is disturbed and breaks down, producing several stronger disturbances (not shown) than in the previous case.

6. Experiments with a climatological background flow

The climatological background flow is the zonal and time average of the flow field from the high resolution NCEP analysis from August through October for the years 2000, 2001 and 2002. The evolution of ITCZ breakdown is shown in Fig. 14 on isentropic level 315 K, which intersects the PV maximum in the lower troposphere.

The strength of the PV strip and the speed of breakdown are similar qualitatively to those of the control run in Fig. 5, with several minor differences. Firstly, the horizontal advection by the background flow is quite noticeable. The produced disturbances are advected westward for more than 40° longitude before they dissipate, by day 18. Secondly, during the breaking process, the PV strip is not able to pool into three (almost) axisymmetric vortices, rather it gets bent into a wavy shape. After breaking, the produced disturbances are considerably smaller and dissipate faster than those in the

control case in Fig. 5.

The southeasterly flow from the SH appears to play an important role in the present case. In the control run (Fig. 5), strong westerlies get induced on the equatorward side of the ITCZ. This flow develops a southerly component and then crosses the equator as northeasterly flow around $+20^\circ$ relative longitude on day 7. It creates a region of anticyclonic flow south of the ITCZ and helps spin up the vortex at the southern edge of the ITCZ. However, with the climatological background flow, the southeasterly flow from the SH overcomes the northeasterly component of the control case. Thus, instead of the spinning effect, the PV strip is facing opposing flow at the eastern end of the equatorward edge. As time advances, the disturbances will be destroyed in this climatological flow. The results of this experiment suggest that the lifetime of the produced disturbances may be shorter when this climatological background flow is present. From this, one might conclude that disturbances produced by ITCZ breakdown in the real atmosphere may be small since the background flow may be unfavorable. However, during times when the background flow is not unfavorable, this may be an important mechanism of pooling vorticity in the tropical east Pacific into disturbances that may subsequently grow given other favorable environmental conditions.

Indeed, we find that longitudinal variations of the background flow are very important for ITCZ breakdown in one additional experiment where we applied the same data as constitutes the climatological background flow, but *before* averaging in longitude. The

results for this three dimensional background flow are shown in Fig. 15. Panels a, b and c depict PV and horizontal wind on days 5, 7 and 9 as in previous figures depicting the evolution in the lower troposphere. Figure 15d shows the same fields on day 0 and thus depicts the background flow field in this case. Note that the x-axis corresponds to actual longitude. Evolution of ITCZ breakdown is considerably faster in this case. Already by day 5 (Fig. 15a), when the forcing is turned off, we see pooling of vorticity on the west side of the PV strip. A sizable vortex has already broken off the western end by day 7 and by day 8 (not shown) the ITCZ has broken into three vortices that may be seen on Fig. 15c, which shows conditions a day later on day 9. The fact that the breaking starts from the western end is especially encouraging in light of the observational case shown in Fig. 10 and other observational cases from the tropical Pacific that will be discussed in future work.

7. Concluding remarks

We have simulated ITCZ breakdown in a three-dimensional PE model with increasingly complex background flows. The heating induced PV anomaly is positive in the lower troposphere and leads to a reversal of the PV gradient on the poleward side of the heating. The lower tropospheric PV anomaly plays the primary role in flow development. The background flow may destabilize or stabilize the ITCZ, depending on whether it reinforces or acts against the PV induced unstable flow, respectively. The deep-heating

induced PV anomaly is negative in the upper troposphere, of larger horizontal extent than that in the lower troposphere, leading to a PV gradient reversal on the equatorward side of the heating where f is smaller.

This process for pooling vorticity in the tropical atmosphere may be particularly important in the tropical east Pacific, where unlike conditions over Africa during the active season, the lower tropospheric meridional temperature gradient is small. In the western Pacific, convergent flow associated with the monsoon trough can lead to the formation of easterly waves through wave activity accumulation (Sobel and Bretherton 1999). That is not the case in the east Pacific. Some easterly waves in the east Pacific may be traced back to disturbances coming from the Atlantic. The process of ITCZ breakdown may be of primary importance in those instances where no disturbance can be traced back, and especially when the breakdown occurs away from the central American coast. We emphasize that the intensity of the disturbances formed by ITCZ breakdown is far less than that of tropical cyclones. In order to form tropical cyclones, moist physical processes are of primary importance and those are neglected in the present study. However, ITCZ breakdown may lead to the pooling of vorticity that subsequently may grow by other means into tropical cyclones.

The vertical profile of heating is found to be important for the development of the flow. In particular, we found that a shallow heating profile induces a stronger lower tropospheric PV field, no upper level PV anomaly, and the ITCZ breaks down one day

later than for deep heating. Different background flows have little influence on ITCZ breakdown in this case. Shallow heating has recently been found to be important in the tropical east Pacific in an observational study by Zhang et al (2004).

We find that in order to simulate ITCZ breakdown a minimum horizontal resolution of T106 (1.1° by 1.1°) is required. This is consistent with our experience of analysis products. PV strips corresponding to the ITCZ in the tropical Pacific cannot be found in NCEP/NCAR reanalysis data, which is of horizontal resolution 2.5° by 2.5°. However, we find such PV strips in the high resolution NCEP global tropospheric analysis, which is of horizontal resolution of 1° by 1°. At present, the atmospheric general circulation models (AGCMs) that include moist processes and cloud cumulus parameterization do not support such high spatial resolution, at least in their standard configuration. However, since ITCZ breakdown is independent of cumulus parameterizations it should show up in the AGCMs at horizontal resolution greater than T106.

Acknowledgments.

We thank Ray Zehr for advice and encouragement in the earliest stage of this work, and Scott Fulton for providing the code to compute the vertical transform of the two heating functions. We thank Chidong Zhang, Rosana Nieto Ferreira and three anonymous reviewers for comments on the manuscript. This work was supported by NSF grant ATM-0301800.

References

Agee, E. M., 1972: Note on ITCZ wave disturbances and formation of tropical storm Anna. *Mon. Wea. Rev.*, **100**, 733–737.

Andrews, D. G., 1984: On the stability of forced non-zonal flows. *Quart. J. R. Met. Soc.*, **110**, 657–662.

Avila, L. A. and G. B. Clark, 1989: Atlantic tropical systems of 1988. *Mon. Wea. Rev.*, **117**, 2260–2265.

Charney, J. G., 1963: A note on large-scale motions in the tropics. *J. Atmos. Sci.*, **20**, 607–608.

Dritschel, D. G., 1989: On the stabilization of a two-dimensional vortex strip by adverse shear. *J. Fluid. Mech.*, **206**, 193–221.

Fulton, S. R. and W. H. Schubert, 1985: Vertical normal mode transforms: theory and application. *Mon. Wea. Rev.*, **113**, 647–658.

Gray, W. M., 1968: Global view of the origin of tropical disturbances and storms. *Mon. Wea. Rev.*, **96**, 669–700.

Gu, G. and C. Zhang, 2002: Westward-propagating synoptic-scale disturbances and the ITCZ. *J. Atmos. Sci.*, **59**, 1062–1075.

Guinn, T. A. and W. H. Schubert, 1993: Hurricane spiral bands. *J. Atmos. Sci.*, **50**, 3380–3403.

Hack, J. J., W. H. Schubert, D. E. Stevens, and H.-C. Kuo, 1989: Response of the Hadley circulation to convective forcing in the ITCZ. *J. Atmos. Sci.*, **46**, 2957–2973.

Heckley, W. A. and A. E. Gill, 1984: Some simple analytical solutions to the problem of forced equatorial long waves. *Quart. J. R. Met. Soc.*, **110**, 203–217.

Hoskins, B. J., 1991: Towards a PV-θ view of the general circulation. *Tellus*, **43AB**, 27–35.

Hoskins, B. J., M. E. McIntyre, and A. W. Robertson, 1985: On the use and significance of isentropic potential vorticity maps. *Quart. J. R. Met. Soc.*, **111**, 877–946.

Hoskins, B. J. and A. J. Simmons, 1975: A multi-layer spectral model and the semi-implicit method. *Quart. J. R. Met. Soc.*, **101**, 637–635.

Joly, A. and A. J. Thorpe, 1990: Frontal instability generated by tropospheric potential vorticity anomalies. *Quart. J. R. Met. Soc.*, **116**, 525–560.

Kasahara, A. and K. Puri, 1981: Spectral representation of three-dimensional global data by expansion in normal mode functions. *Mon. Wea. Rev.*, **109**, 37–51.

Kuo, H. L., 1973: Dynamics of quasi-geostrophic flows and instability theory. *Adv. Appl. Mech.*, **13**, 247–330.

Lawrence, M. B., L. A. Avila, J. L. Frankin, R. J. Pasch, and S. R. Stewart, 2001: Eastern north Pacific hurricane season of 2000. *Mon. Wea. Rev.*, **129**, 3004–3014.

Liu, W. T. and X. Xie, 2002: Double intertropical convergence zones - a new look using scatterometer. *Geophys. Res, Lett.*, 29(22),2072,doi:10.1029/2002GL015431.

Nesbitt, S. W. and D. J. C. E. J. Zipser, 2000: A census of precipitation features in the tropics using TRMM: Radar, ice scattering, and lightning observations. *J. Climate.*, **13**, 4087–4106.

Nieto Ferreira, R. and W. H. Schubert, 1997: Barotropic aspects of ITCZ breakdown. *J. Atmos. Sci.*, **54**, 261–285.

Schubert, W. H., P. E. Ciesielski, D. E. Stevens, and H.-C. Kuo, 1991: Potential vorticity modeling of the ITCZ and the Hadley circulation. *J. Atmos. Sci.*, **48**, 1493–1509.

Sobel, A. H. and C. S. Bretherton, 1999: Development of synoptic-scale disturbances over the summertime tropical northwest Pacific. *J. Atmos. Sci.*, **56**, 3106–3127.

Thompson, O. E. and J. Miller, 1976: Hurricane Carmen: August-September 1974–Development of a wave in the ITCZ. *Mon. Wea. Rev.*, **104**, 656–659.

Wu, Z., 2003: A shallow CISK, deep equilibrium mechanism for the interaction between large-scale convection and large-scale circulations in the tropics. *J. Atmos. Sci.*, **60**, 377–392.

Zehnder, J. A. and D. M. Powell, 1999: The interaction of Easterly waves, orography, and the Intertropical Convergence Zone in the genesis of Eastern Pacific tropical cyclones. *Mon. Wea. Rev.*, **127**, 1566–1585.

Zhang, C., M. McGauley, and N. A. Bond, 2004: Shallow meridional circulation in the tropical eastern Pacific. *J. Climate*, **17**, 133–139.

List of Figures

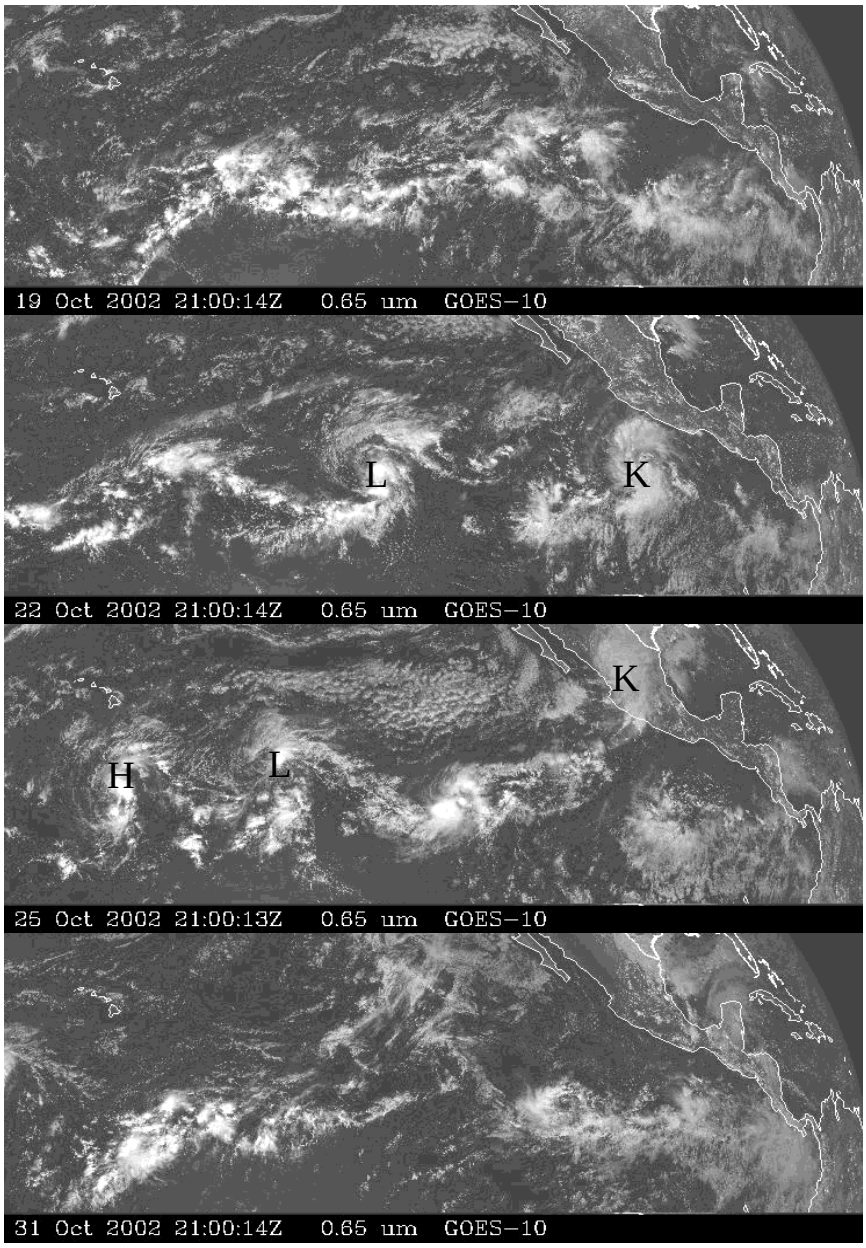

Figure 1: GOES-10 visible images taken in October 2002 covering the area 0° –30° N latitude and 170° W–60° W longitude, which includes the tropical east Pacific. The ITCZ was located at approximately 10°N on the 19th. It undulated and subsequently broke down on the 22nd. The labeled cloud clusters are hurricane Kenna (K, 22-26 October), tropical cyclone Lowell (L, 22-31 October) and hurricane Huko (H, 10/24-11/03). At the end of October, a new ITCZ reformed.

(a) Horizontal profile

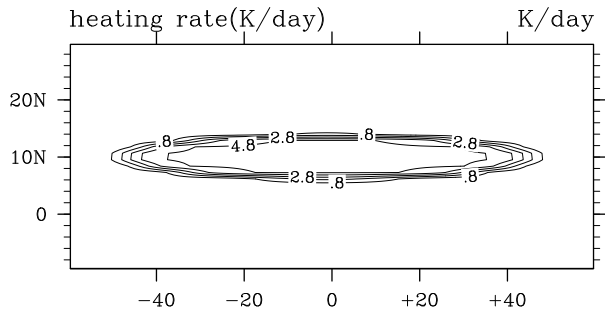

(b) Vertical profile

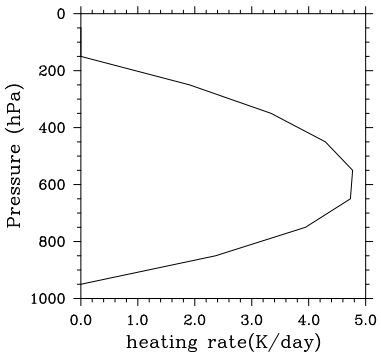

Figure 2: (a) Horizontal profile of the prescribed heating at the level of maximum heating. The X-axis is longitude, relative to the center, the Y-axis is latitude. The heating is elliptic and spans 90° longitude and 10° latitude, centered at 10° N at each level. Contour interval is 1 K/day. (b) Vertical profile of the heating in K/day. The heating rate is strongest (about 4.8 K/day) at 600 hPa and decreases to zero at 150 hPa and 950 hPa.

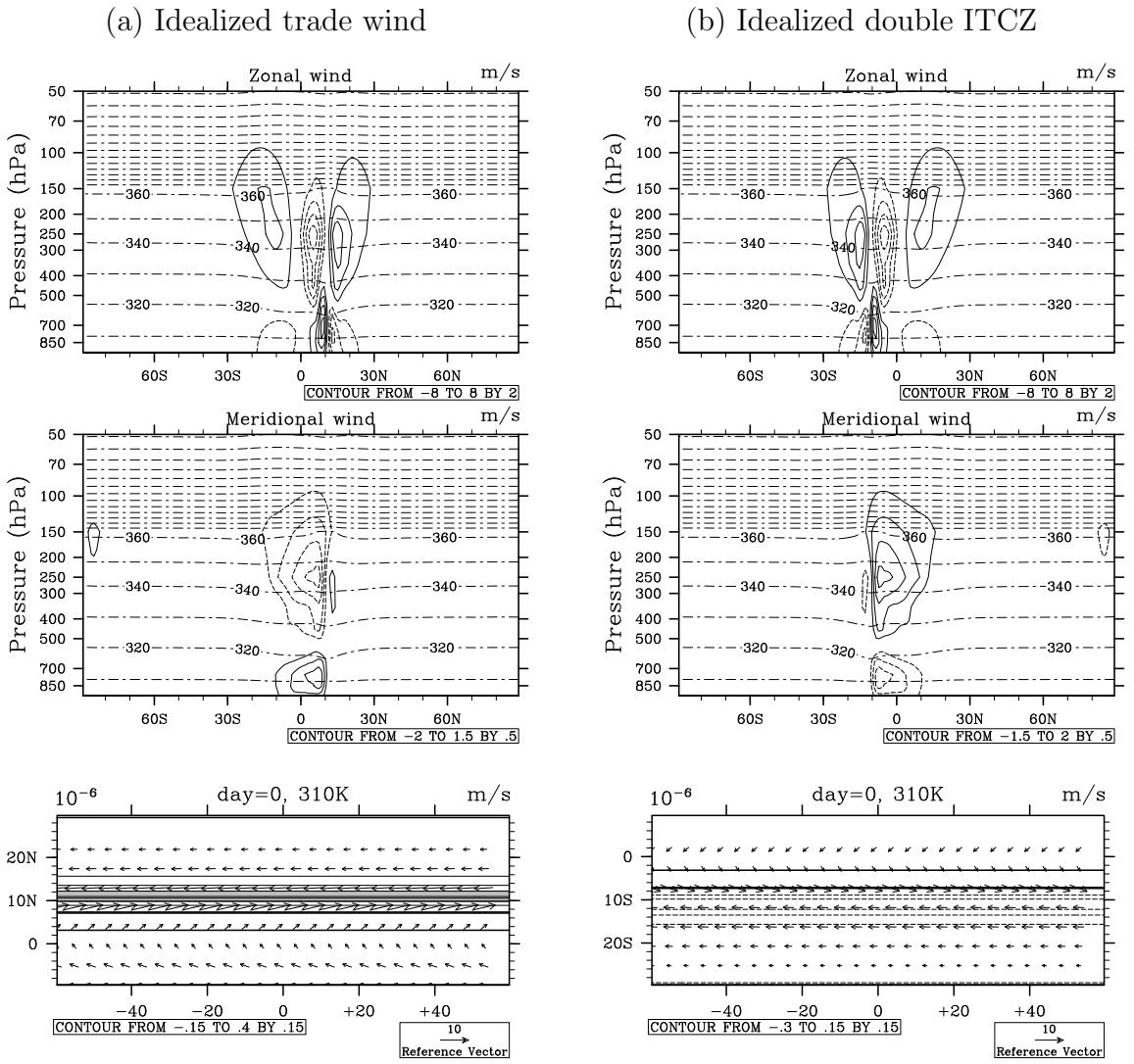

Figure 3: Background flow for (a) the idealized trade wind case and (b) the double ITCZ case. Shown are (from top to bottom) zonal wind, meridional wind, and both components of the wind with PV contoured on the 310 K surface. The dash-dotted contours in the top two panels indicate isentropic surfaces with contour interval of 10 K. The contour interval for zonal wind is 2 m/s, and 0.5 m/s for meridional wind. Solid contours indicate positive values, dashed negative and the heavy contour is zero. The reference arrow at the bottom indicates a value of 10 m/s, the PV contour interval is 0.15 PVU.

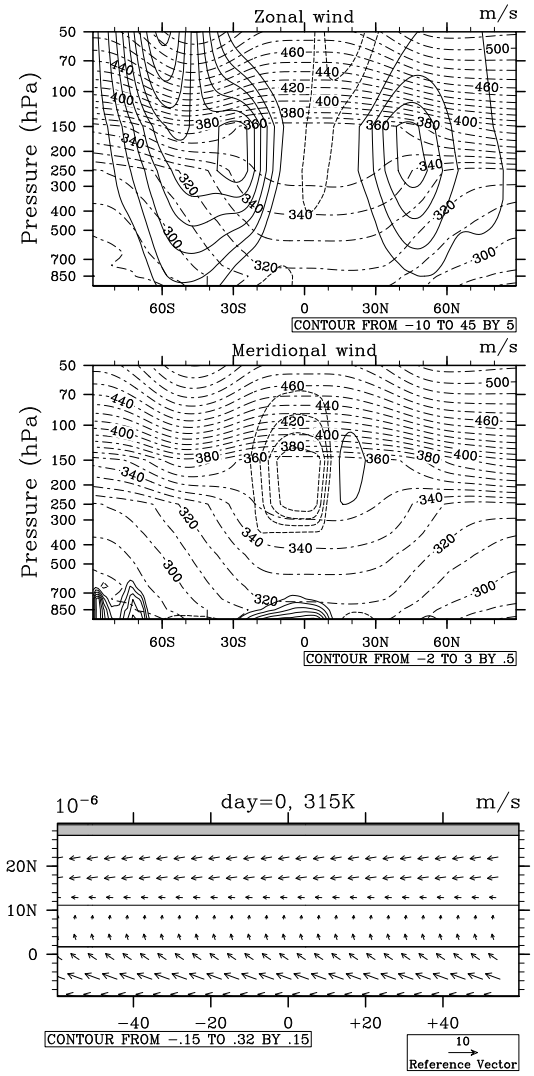

Figure 4: Same as Fig. 3 except for the background flow derived from high resolution NCEP global tropospheric analyses from August through October of 2000–2002. The contour interval for the zonal wind component (top) is 5 m/s and 0.5 m/s for the meridional wind component (center). The zero contour is heavy, and dashed contours depict negative value. The bottom diagram shows the horizontal wind on the 315 K isentropic surface with PV contoured every 0.15 PVU.

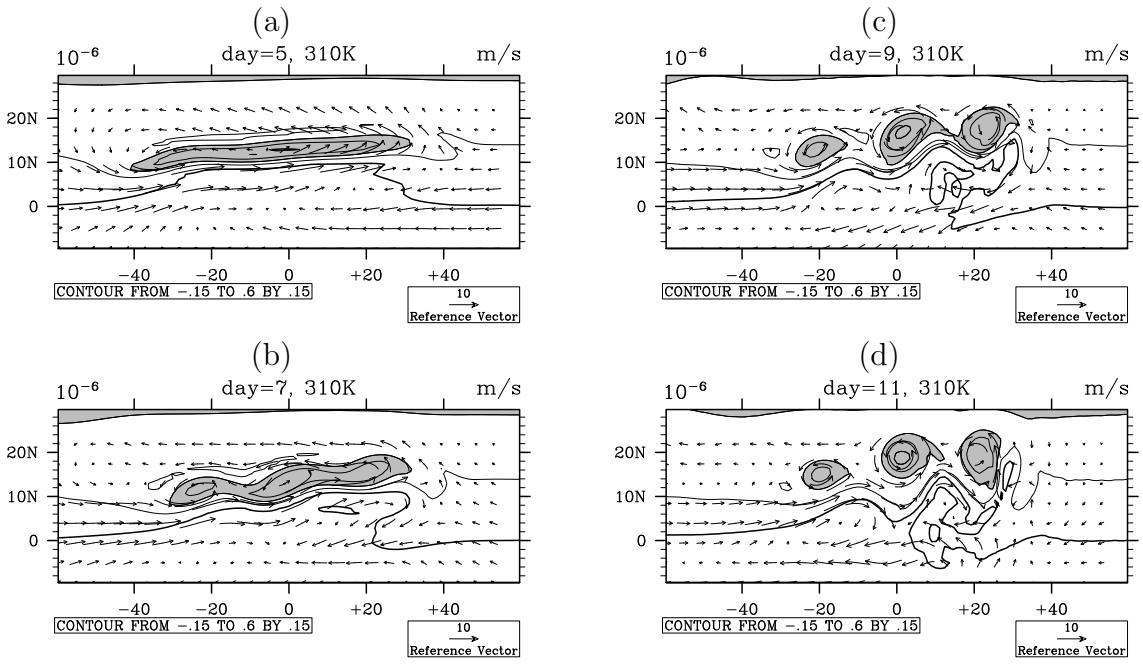

Figure 5: PV and horizontal wind on the 310 K isentropic surface for the simulation in a background state of rest on days 5, 7, 9 and 11 (a, b, c, d, respectively. The X-axis is relative longitude, the Y-axis is latitude from 10° S to 30° N. The 310 K surface is located close to 800 hPa. Contours depict PV and vectors are the corresponding wind field. The solid contours indicate positive PV, dashed negative PV and the heavy contour is zero. The contour interval is 0.15 PVU. Areas where PV values are greater than 0.3 PVU are shaded. The reference wind vector is 10 m/s.

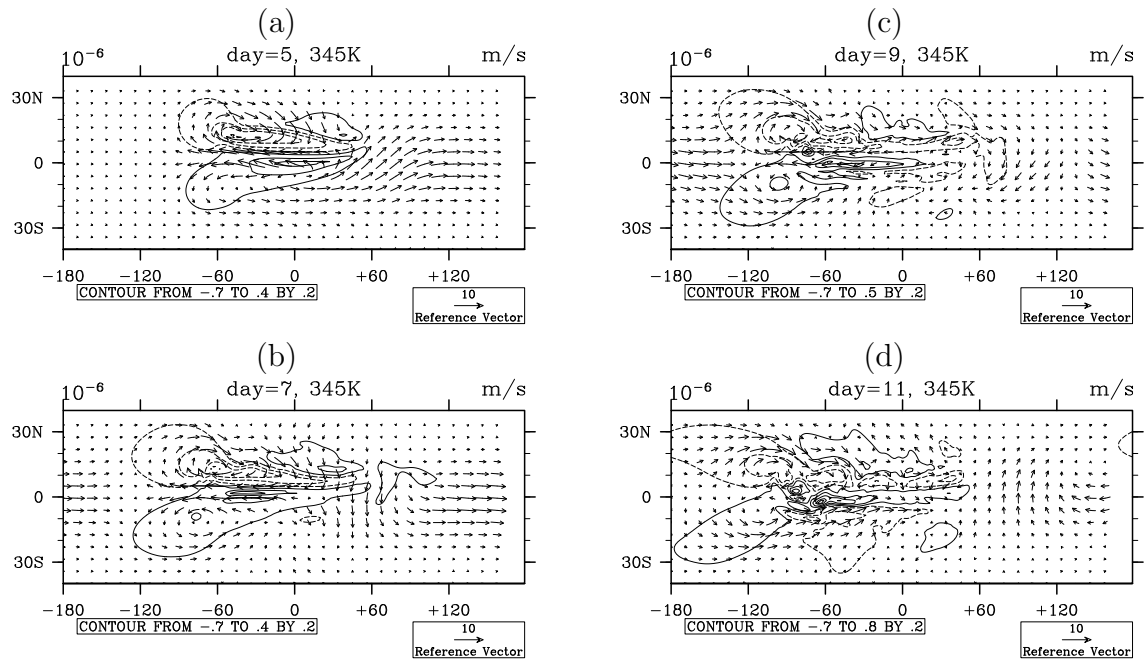

Figure 6: PV anomaly and horizontal wind on the 345 K isentropic surface, which is close to the 250 hPa pressure level, on days 5, 7, 9 and 11 (a, b, c, d, respectively). The region shown here is 40° S–40° N and all longitudes. The contour interval is 0.2 PVU and the zero contour is suppressed. The reference vector indicates wind speed of 10 m/s.

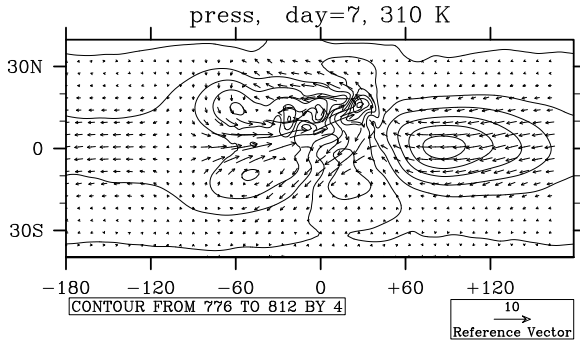

Figure 7: Pressure and wind on the 310 K isentropic surface on day 7 for the simulation in a background state of rest. The contour interval is 4 hPa, the reference vector indicates a wind speed of 10 m/s.

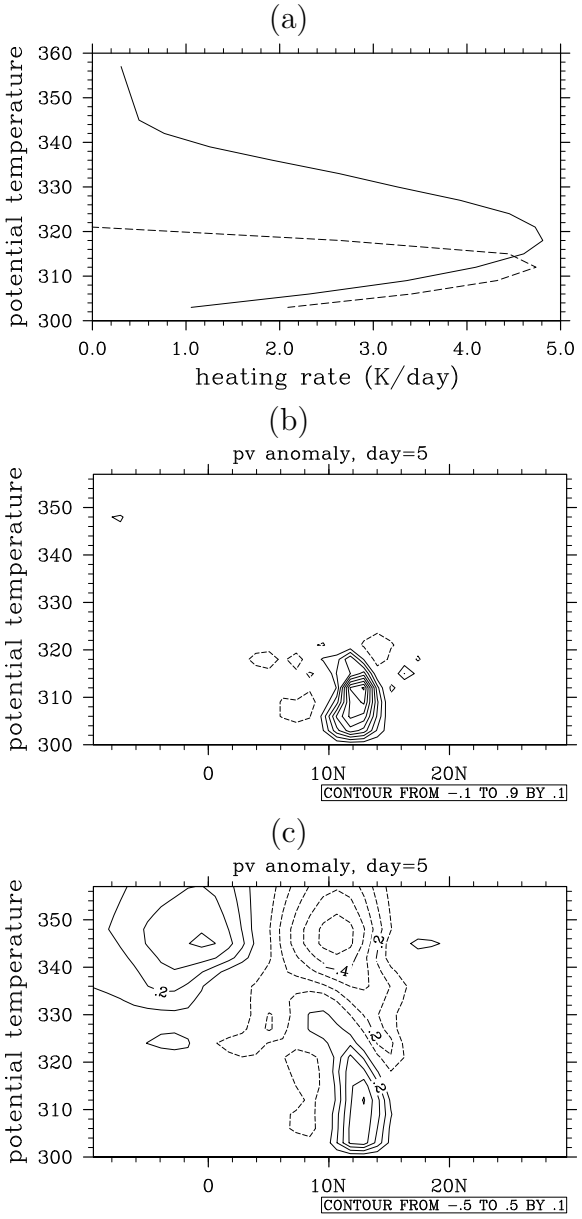

Figure 8: (a) Heating rate (K/day) for shallow (dashed) and deep (solid) heating. The vertical coordinate is potential temperature. (b) and (c) show meridional cross-sections (latitude and potential temperature) through the center of the PV anomalies (PV on day 0 subtracted from PV on day 5) generated by shallow and deep heating, respectively. Contour interval is 0.1 PVU. Solid/dashed contours indicate a positive/negative PV anomaly, the zero contour is suppressed.

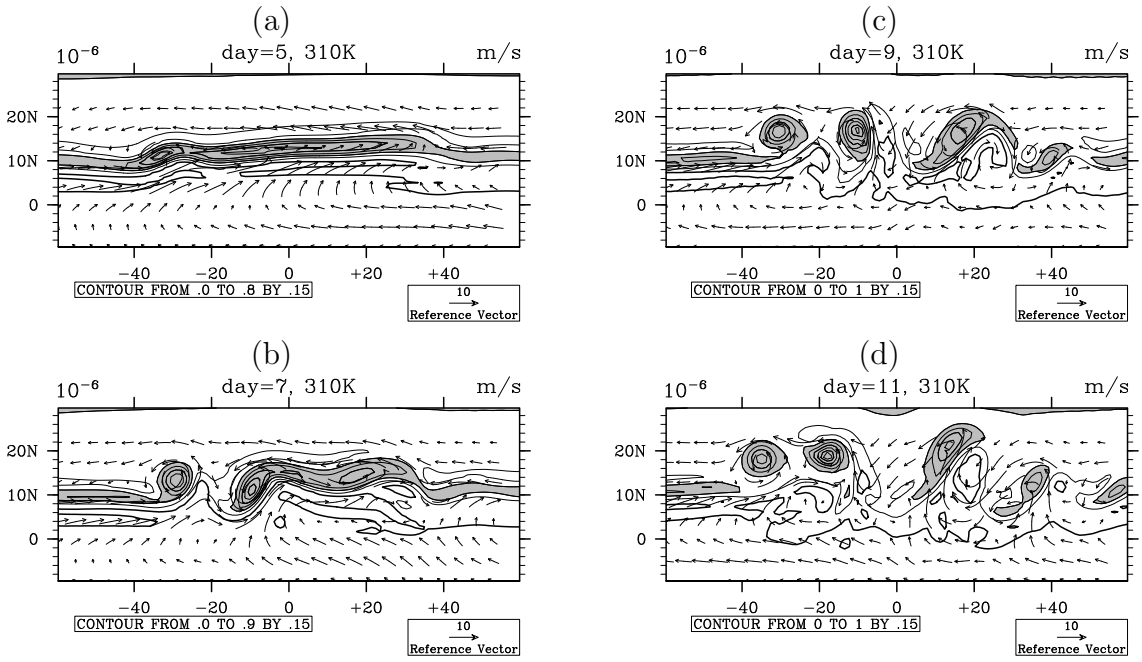

Figure 9: Same as Fig. 5 except for the idealized trade wind background flow.

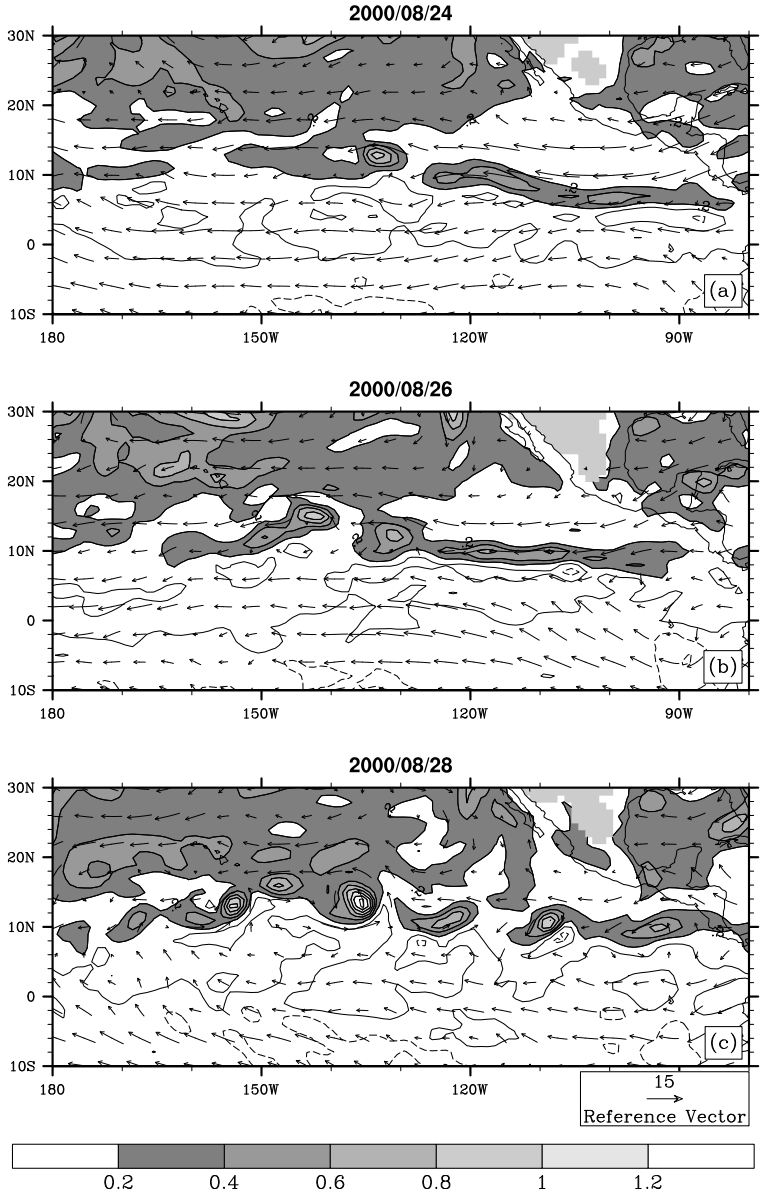

Figure 10: A case of ITCZ breakdown observed at the end of August 2000. (a) An elongated PV strip is located in the tropical East Pacific on 24 August. Its length is about 40° longitude. The disturbance located near 12.5°N, 135°W broke off from the western end of the PV strip on 26 August (b) and developed into a named tropical cyclone, John (8/28–9/01). (c) The PV field on 28 August. The remaining part of the ITCZ continued breaking into a series of small disturbances. Contour interval is 0.2 PVUs.

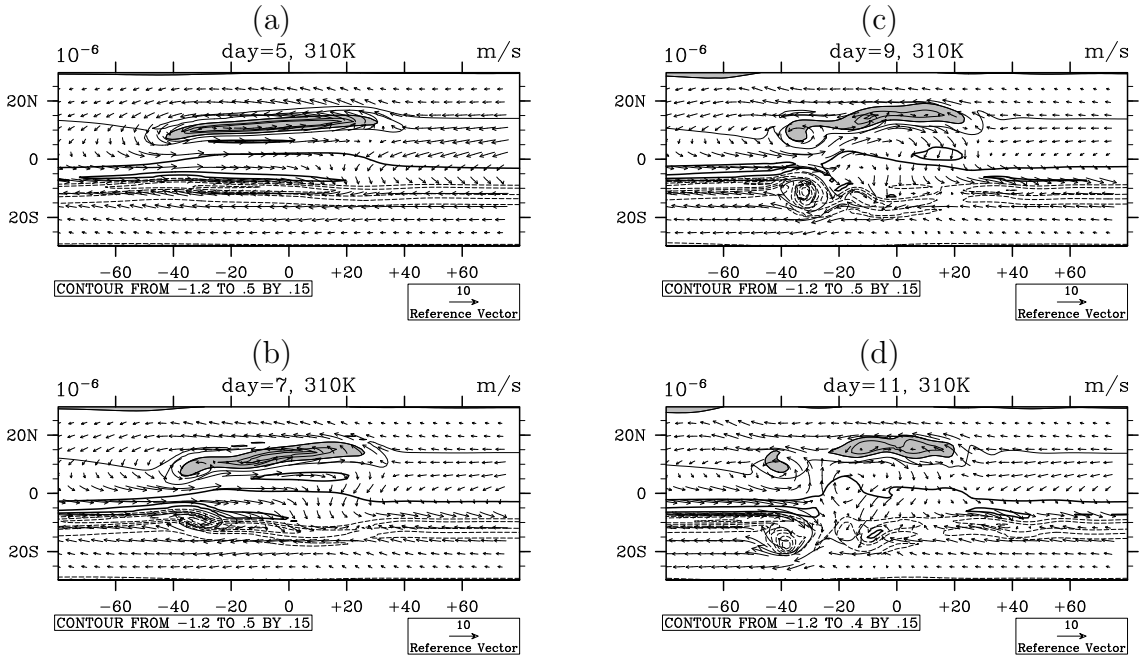

Figure 11: Same as Fig. 5 except for the idealized double ITCZ background flow and for an extended domain.

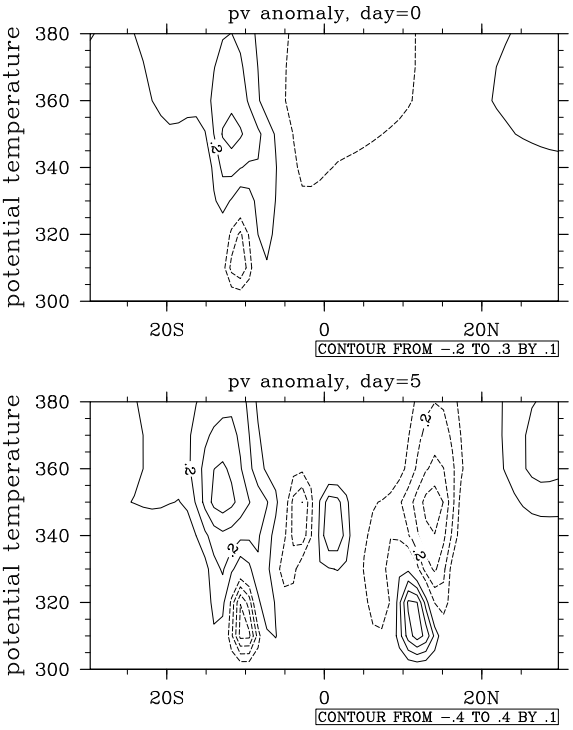

Figure 12: Meridional cross section (latitude vs potential temperature) through the center of the ITCZ PV anomaly for the case of deep ITCZ heating in a double ITCZ background flow. PV anomaly (subtract PV on day 0 in the background state of rest from the PV field) on day 0 (a) and on day 5 (b). Contour interval is 0.1 PVU with the zero contour suppressed.

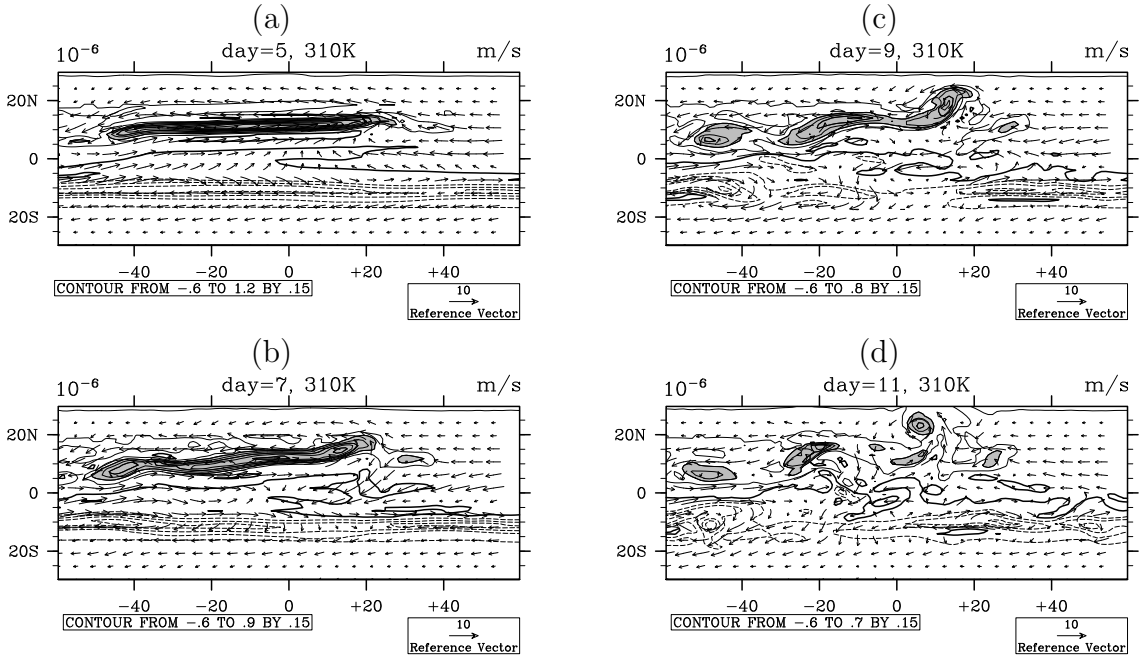

Figure 13: Same as Fig. 11 except the prescribed heating is shallow.

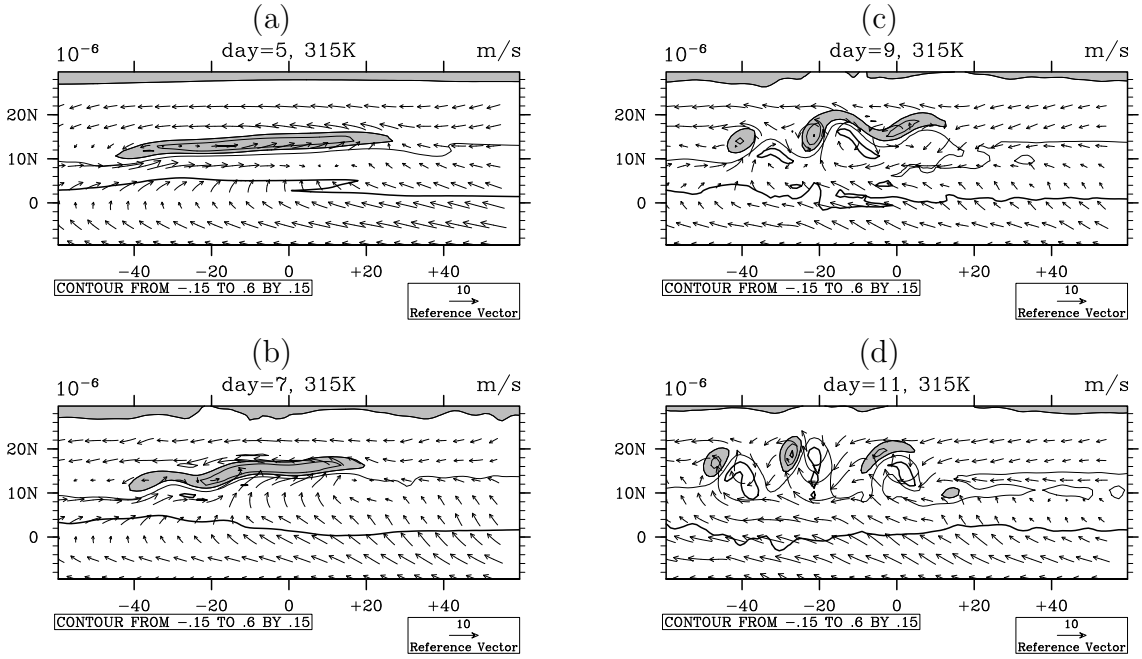

Figure 14: Same as Fig. 5 except for the climatological background flow, and the isentropic surface is 315 K.

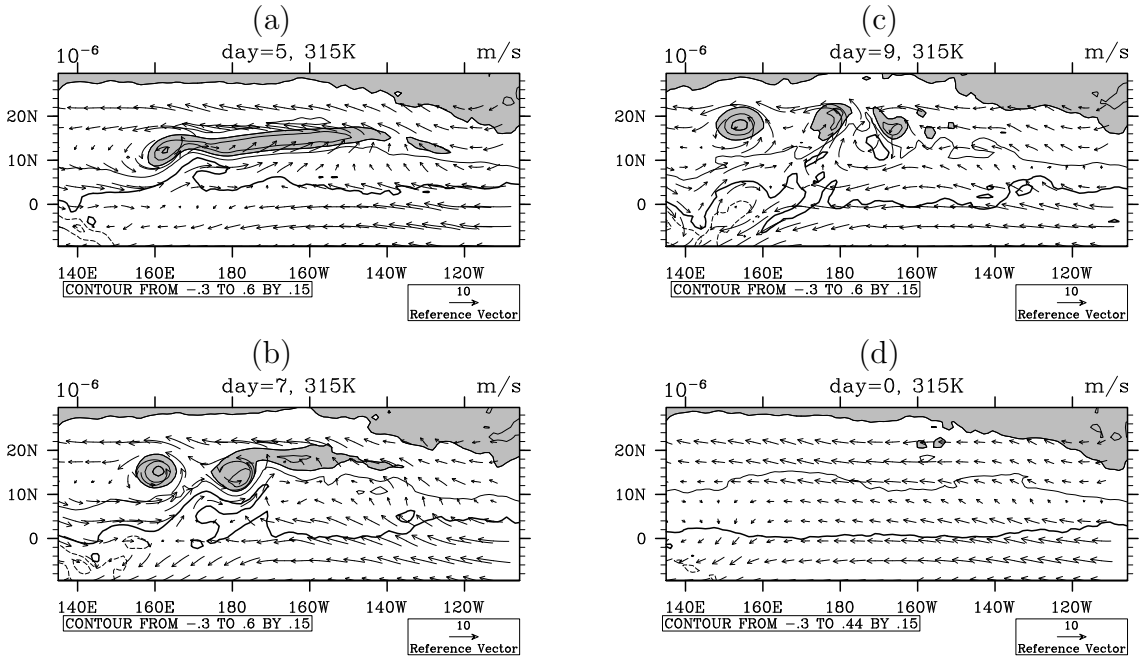

Figure 15: Same as Fig. 14 except for the three dimensional climatological background flow. (a) shows results on day 5, (b) on day 7, (c) on day 9 and (d) on day 0. Note that in this case the x-axis is actual longitude from 135° E to 105° W.